ISSN 1063-7788, Physics of Atomic Nuclei, 2018, Vol. 81, No. 5, pp. 575–582. © Pleiades Publishing, Ltd., 2018.
Original Russian Text © A.V. Glushkov, M.I. Pravdin, A.V. Saburov, 2018, published in Yadernaya Fizika, 2018, Vol. 81, No. 5, pp. 535–542.

ELEMENTARY PARTICLES AND FIELDS
Experiment

Energy Spectrum of Ultrahigh-Energy Cosmic Rays according to Data from Ground-Based Scintillation Detectors of the Yakutsk EAS Array

A. V. Glushkov[1)*], M. I. Pravdin[1)], and A. V. Saburov[1)]

Received December 27, 2017

Abstract—Results obtained from an analysis of the energy spectrum of cosmic rays with energies in the region of $E_0 \geqslant 10^{17}$ eV over the period of continuous observations from 1974 to 2017 are presented. A refined expression for estimating the primary-particle energy is used for individual events. This expression is derived from calculations aimed at determining the responses of the ground-based and underground scintillation detectors of the Yakutsk array for studying extensive air showers (EAS) and performed within the QGSJET-01-d, QGSJET-II-04, SIBYLL-2.1, and EPOS-LHC models by employing the CORSIKA code package. The new estimate of E_0 is substantially lower than its counterpart used earlier.

DOI: 10.1134/S106377881804004X

1. INTRODUCTION

The energy spectrum of ultrahigh-energy cosmic rays (CR) ($E_0 \geqslant 10^{17}$ eV) is one of the key links in the chain of problems on the path toward obtaining deeper insight into the nature of primary particles that have such energies. Experimental results obtained at different arrays for studying extensive air showers (EAS) [1–7] differ in absolute intensity nearly by a factor of two but are close in shape [8]. This situation is due largely to the fact that, at the majority of large arrays worldwide, use is made of different methods for determining the primary-particle energy E_0 in view of the difference of the procedures for EAS detection at these arrays. Here, one cannot dispense with invoking theoretical ideas of the development of EAS.

The Yakutsk EAS array is the oldest in the world. It has operated continuously since 1974, standing out among the other large arrays owing to its multifunctionality—specifically, the ability to measure simultaneously all EAS particles with ground-based scintillation detectors of area 2 m^2, muons at a threshold above $1.0\sec\theta$ GeV with analogous underground detectors, and Cherenkov light from EAS. The Cherenkov component carries information about approximately 80% of the primary energy scattered by a shower in the Earth's atmosphere and makes it possible to determine E_0 calorimetrically [9–12]. For the first time ever, this method was applied in [13] at energies around 10^{15} eV. At the Yakutsk EAS array, it was implemented in the energy range of $E_0 \approx (1.0-100) \times 10^{17}$ eV and the zenith-angle range of $\theta \leqslant 45^\circ$ [9]:

$$E_0 = (4.1 \pm 1.4) \times 10^{17} (S_{600}(0^\circ))^{0.97\pm0.04} \text{ [eV]}, \quad (1)$$

$$S_{600}(0^\circ) = S_{600}(\theta)\exp((\sec\theta - 1)1020/\lambda) \text{ [m}^{-2}\text{]}, \quad (2)$$

$$\lambda = 400 \pm 45 \text{ g/cm}^2. \quad (3)$$

Here, $S_{600}(\theta)$ is the particle density measured by ground-based scintillation detectors at the distance of $R = 600$ m from the shower axis. Later, relations (1) and (3) changed somewhat to become [10–12]

$$E_0 = (4.8 \pm 1.6) \times 10^{17} (S_{600}(0^\circ))^{1.0\pm0.02} \text{ [eV]}, \quad (4)$$

$$\lambda = (450 \pm 44) + (32 \pm 15)\log(S_{600}(0^\circ)) \text{ [g/cm}^2\text{]}. \quad (5)$$

The cosmic-ray energy spectrum estimated on the basis of expression (4) proved to be substantially higher in intensity than all data obtained worldwide. In [14, 15], we revisited the energy calibration of showers by means of the CORSIKA code [16] on the basis of modern hadron-interaction models considered below.

2. EVALUATING PRIMARY ENERGY

2.1. Data on Lateral Distribution from Scintillation Detectors

Basic parameters of EAS at the Yakutsk EAS array (such as arrival direction, coordinates of the

[1)] Shafer Institute of Cosmophysical Research and Aeronomy, Siberian Branch, Russian Academy of Sciences, pr. Lenina 31, Yakutsk, 677980 Russia.
[*] E-mail: a.v.glushkov@ikfia.ysn.ru

axis, and primary energy) are determined with the aid of the lateral distribution of all particles (electrons, muons, and high-energy photons) recorded by ground-based scintillation detectors. These particles traverse a multilayered shield from snow, iron, wood, and duralumin (the total thickness is about 2.5 g/cm^2) and thereupon a scintillator 5 cm thick (its density is 1.06 g/cm^3), where they deposit some energy $\Delta E_s(R)$, which is proportional to the number of particles that traversed the detector. In practice, this energy deposition is measured in relative units; that is,

$$\rho_s(R) = \Delta E_s(R)/E_1\ [\mathrm{m}^{-2}], \qquad (6)$$

where $E_1 = 11.75$ MeV is the energy deposited in a ground-based detector upon the passage through it of one vertical relativistic muon (unit response).

The scintillation detectors are calibrated and are controlled with the aid of the amplitude density spectra from background cosmic-ray particles [17]. In doing this, use is made of integrated spectra of two types. Of them, the first is the spectrum from one of the detectors controlled by the neighboring detector from the same station (spectrum of "double coincidences" with a frequency of about 2 to 3 s^{-1}). The second is a spectrum without a control; the respective frequency is about 200 s^{-1}. It is used to calibrate muon detectors. Both spectra have a power-law form; that is,

$$F(>\rho) \sim \rho^{-\eta} \sim U^{-\eta}, \qquad (7)$$

where $\eta = 1.7$ and 3.1 in, respectively, the first and the second case and $\rho = U/U_1$ is the particle density in units of the amplitude U_1 of the signal of the reference detector from vertical relativistic cosmic muons. The procedure of calibration and control reduces to monitoring the quantity U_1 for all detectors by periodically measuring their density spectra. This is done once per two days, the double-coincidence spectra and spectra without control being taken for two hours and 30 minutes, respectively.

We have calculated lateral distributions of responses on the basis of the QGSJET-01-d [18], QGSJET-II-04 [19], SIBYLL-2.1 [20], and EPOS-LHC [21] models for primary protons and iron nuclei in the range of energies between $10^{17.0}$ and $10^{19.5}$ eV for various zenith angles. As a model for low energies, we took FLUKA [22]. First, we calculated the responses $u_k(E,\theta)$ to single particles of type k (here, k is an electron, a muon, or a photon) with energy E. In doing this, we took into account all processes of energy deposition and absorption in the shield and in the scintillator and the cross sections for the interactions undergone by these particles. After that, the development of EAS in the real atmosphere

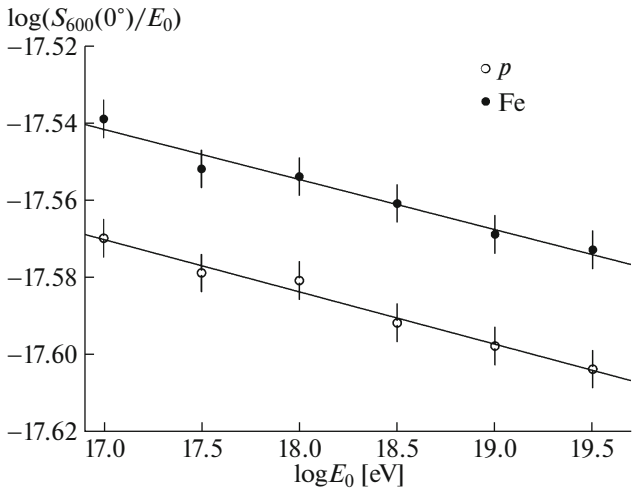

Fig. 1. $\log(S_{600}(0^\circ)/E_0)$ as a function of the energy E_0 for primary (open circles) protons and (closed circles) iron nuclei in vertical showers according to the QGSJET-01-d model. The curves represent linear approximations of the experimental points.

was simulated with the aid of the CORSIKA code. Five hundred showers were generated for each set of primary parameters (including primary-particle mass, primary energy, and zenith angle). With the aim of reducing the computer time, we invoked the statistical-thinning mechanism, its parameters being $E_i/E_0 = 10^{-5}$ and $w_{\max} = 10^4$. A rescale to the density was accomplished upon taking into account the number of particles per detector of given area. Averaging over respective showers was performed, and the energy spectra $d_k(E,R,\theta)$ were calculated for all types of particles in the intervals ($\log R_j$, $\log R_j + 0.04$) of distances. The signal in (6) was determined by the sum of the responses; that is,

$$\rho_s\,(R) = \sum_{k-1}^{3}\sum_{i=1}^{I_k} u_k(E_i,\theta_i) d_k\,(E_i,R,\theta_i)\,, \qquad (8)$$

where I_k is the number of particles that belong to type k and which hit the detector.

Figure 1 shows $\log(S_{600}(0^\circ)/E_0)$ as a function of E_0 for primary (open circles) protons and (closed circles) iron nuclei according to calculations on the basis of the QGSJET-01-d model. These values satisfy the relation

$$E_0 = (3.55 \pm 0.1) \times 10^{17} (S_{600}(0^\circ))^{1.02}\ [\mathrm{eV}]. \qquad (9)$$

The estimates based on the application of the QGSJET-II-04, EPOS-LHC, and SIBYLL-2.1 models are, respectively,

$$E_0 = (3.19 \pm 0.1) \times 10^{17} (S_{600}(0^\circ))^{1.03}\ [\mathrm{eV}], \qquad (10)$$

$$E_0 = (2.87 \pm 0.1) \times 10^{17} (S_{600}(0^\circ))^{1.03}\ [\mathrm{eV}], \qquad (11)$$

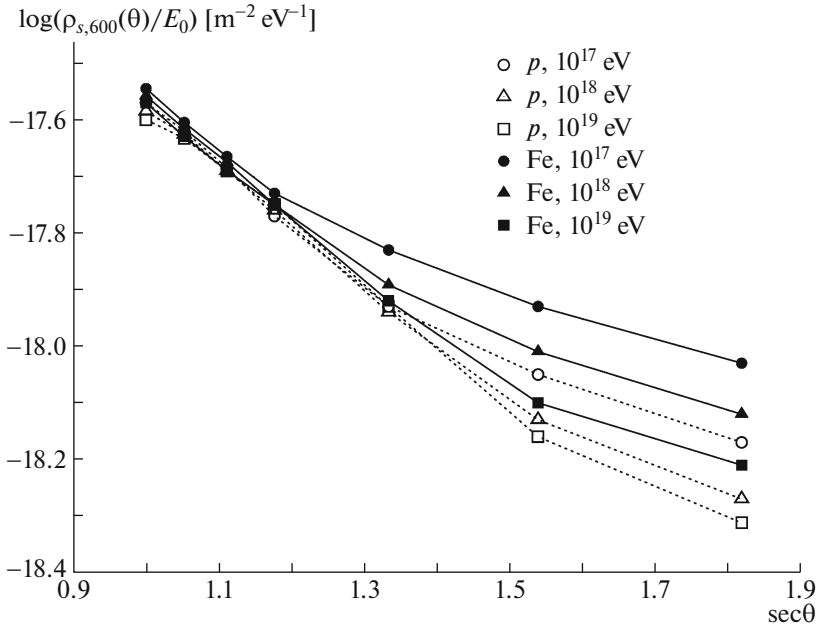

Fig. 2. $\log(S_{600}(\theta)/E_0)$ as a function of the zenith angle according to calculations performed on the basis of the QGSJET-01-d model for primary (open symbols) protons and (closed symbols) iron nuclei of energy $E_0 =$ (open and closed circles) 10^{17}, (open and closed triangles) 10^{18}, and (open and closed boxes) 10^{19} eV. The points on display were connected by lines in order to guide the eye.

$$E_0 = (3.72 \pm 0.1) \times 10^{17} (S_{600}(0^\circ))^{1.02} \text{ [eV]}. \quad (12)$$

Figure 2 gives $\log(S_{600}(\theta)/E_0)$ as a function of the zenith angle according to calculations on the basis of the QGSJET-01-d model. This dependence corresponds to the variations in λ in (2) that are shown in Fig. 3. The dashed curve in Fig. 3 represents absorption ranges for a mixed composition of primary nuclei according to our experimental data from [23, 24]. The dotted curve corresponds to the empirical relation (5).

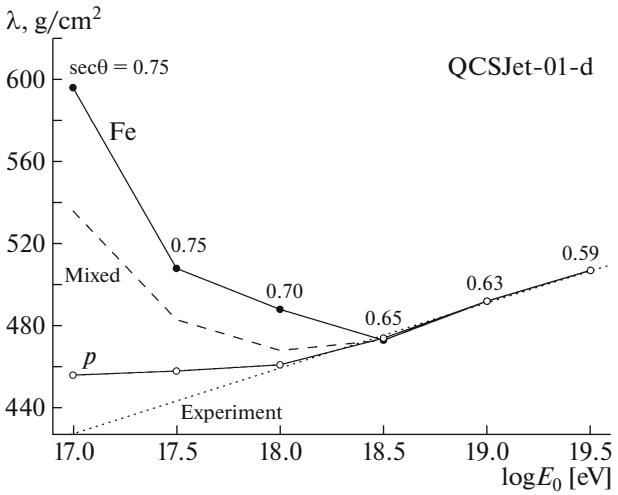

Fig. 3. Absorption ranges in (2) upon rescaling $S_{600}(\theta)$ from inclined to vertical showers according to the QGSJET-01-d model for primary protons (p), mixed composition, and iron nuclei (Fe) versus E_0. The numbers indicate the limiting admissible zenith angles. The dotted curve represents relation (5).

2.2. Data Obtained Calorimetrically

The method in question is described here by considering the example of experimental data from [9, 10] taken as the basis in developing a calorimetric method for estimating E_0 at the Yakutsk EAS array. Tables 1 and 2 give observed parameters and basic constituents of $E_0 = 10^{18}$ eV in showers characterized by $\cos\theta = 0.95$. The "average p-Fe" line corresponds to values averaged over the CR composition and over all models. The electron–photon component energy scattered in the atmosphere is

$$E_i = E_\gamma + E_{\text{ion}}, \quad (13)$$

where E_γ is the gamma-ray energy at the observation level and E_{ion} is the total ionization loss of all electrons. This loss is proportional to the total flux of Cherenkov light, F, in the atmosphere; that is,

$$E_i = kF, \quad (14)$$

where

$$k = k_\gamma + k_{\text{ion}} \quad (15)$$
$$= (E_\gamma + E_{\text{ion}})/F \text{ [eV/photon eV}^{-1}\text{]}.$$

Table 1. Observed parameters of EAS characterized by $E_0 = 10^{18}$ eV and $\cos\theta = 0.95$ and initiated by primary nuclei (A) according to the CORSIKA code [16] and according to the experiments reported in [9, 10]

Model	A	$k_\gamma(\theta)$, eV^2 ($\times 10^4$)	$k_{\rm ion}(\theta)$, eV^2 ($\times 10^4$)	$F(\theta)$, eV^{-1} ($\times 10^{13}$)	$N_s(\theta)$ ($\times 10^8$)	$S_{600}(\theta)$, m^{-2}	$N_\mu(\theta)$ ($\times 10^6$)
QGSJET-01-d	p	0.341	2.846	2.104	2.178	2.312	5.000
	Fe	0.224	2.910	2.148	1.250	2.432	7.225
QGSJET-II-04	p	0.364	2.816	2.070	2.296	2.438	5.582
	Fe	0.246	2.894	2.148	1.358	2.636	7.777
SIBYLL-2.1	p	0.345	2.822	2.100	2.512	2.193	4.254
	Fe	0.224	2.910	2.228	1.384	2.249	4.930
EPOS-LHC	p	0.377	2.815	2.023	2.355	2.655	5.905
	Fe	0.230	2.894	2.133	1.419	2.917	8.180
Average	p	0.357	2.825	2.074	2.335	2.400	5.185
Average	Fe	0.231	2.902	2.164	1.353	2.558	7.028
Average	p–Fe	0.294	2.864	2.119	1.844	2.479	6.107
Experiment [9, 10]	–	3.700		2.510	1.793	2.656	6.00

Table 2. Energy balance in EAS characterized by $E_0 = 10^{18}$ eV and $\cos\theta = 0.95$ and initiated by primary nuclei (A) according to the CORSIKA code [16] and according to the experiments reported in [9, 10]

Model	A	E_γ, eV ($\times 10^{17}$)	$E_{\rm ion}$, eV ($\times 10^{17}$)	$E_{\rm el}$, eV ($\times 10^{17}$)	E_μ, eV ($\times 10^{17}$)	ΔE, eV ($\times 10^{17}$)	E_0, eV ($\times 10^{17}$)
QGSJET-01-d	p	0.806	6.620	1.469	0.517	0.565	9.978
	Fe	0.529	6.600	1.306	0.785	0.798	9.972
QGSJET-II-04	p	0.859	6.476	1.474	0.547	0.624	9.980
	Fe	0.582	6.430	1.302	0.844	0.866	9.981
SIBYLL-2.1	p	0.909	6.625	1.523	0.428	0.491	9.976
	Fe	0.528	6.679	1.340	0.702	0.716	9.965
EPOS-LHC	p	0.891	6.412	1.482	0.524	0.657	9.966
	Fe	0.543	6.415	1.305	0.794	0.898	9.955
Average	p	0.866	6.533	1.487	0.504	0.584	9.974
Average	Fe	0.546	6.531	1.313	0.781	0.820	9.968
Average	p–Fe	0.706	6.532	1.400	0.643	0.702	9.970
Experiment [9, 10]	–	9.287		0.947	0.636	0.860	11.730
New estimate	–	7.926		0.947	0.618	0.702	10.190

Figure 4 shows the rescaling coefficient in (15) as a function of the distance between the shower-maximum position $X_{\rm max}$ and the observation level $X_{\rm obs} = 1020\sec\theta$ g cm^{-2}. The flux F was found with allowance for its weakening by a factor of 1.15 because of Rayleigh light scattering in the absolutely clean atmosphere and a deterioration of its transparency by a factor of 1.1 for the shower sample from [9, 10]. It is given within a 1-eV radiation interval; that is,

$$F = 1.265F_{\rm obs}/\Delta\varepsilon, \qquad (16)$$

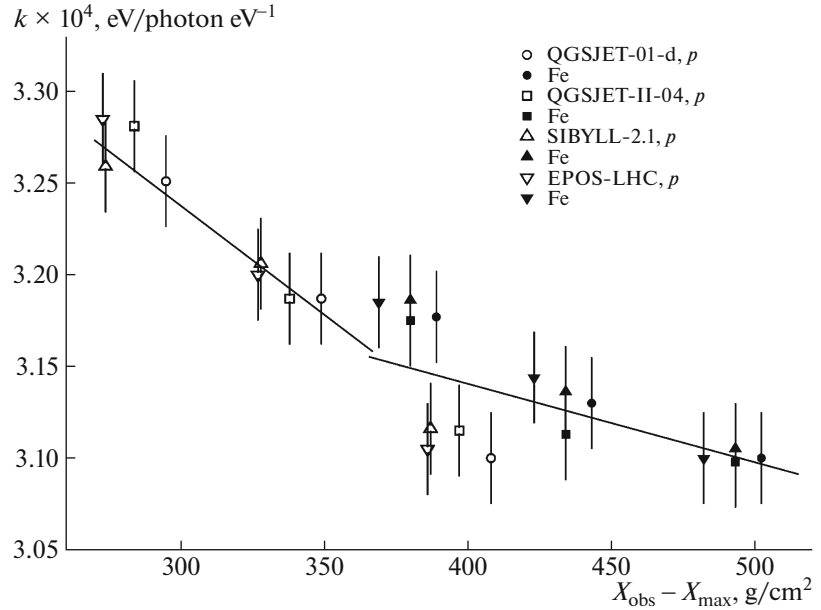

Fig. 4. Rescaling coefficient in (15) as a function of the distance between the shower-maximum position $X_{\max}$ and the observation level $X_{\rm obs} = 1020 \sec\theta$ g cm^{-2} for primary (open symbols) protons and (closed symbols) iron nuclei according to the (open and closed circles) QGSJET-01-d, (open and closed boxes) QGSJET-II-04, (open and closed triangles) SIBYLL-2.1, and (inverted open and closed triangles) EPOS-LHC models. The lines represent approximations.

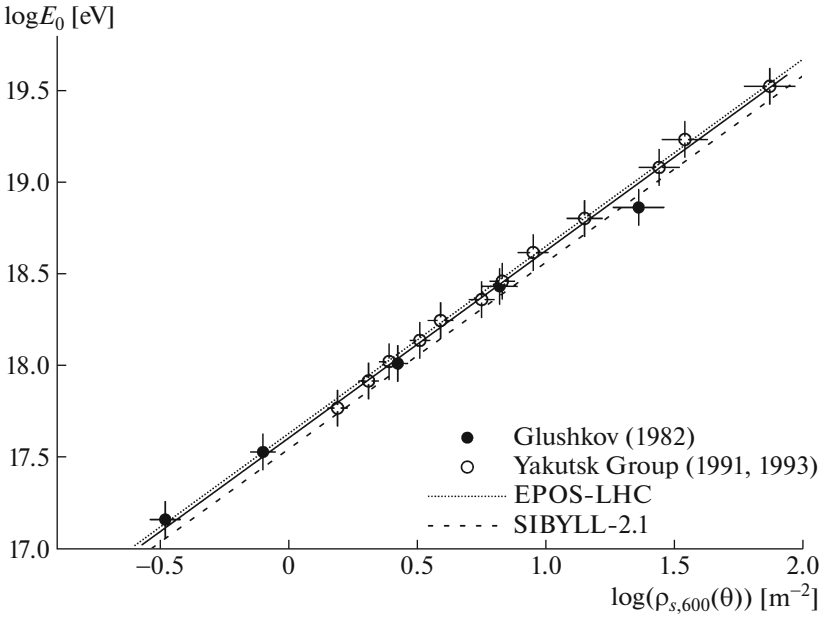

Fig. 5. Primary energy E_0 as a function of the parameter $S_{600}(\theta)$ in showers characterized by $\langle\cos(\theta)\rangle = 0.95$ according to data from (closed circles) [9] and (open circles) [10] upon the application of the new calorimetric procedure (see main body of the text). The solid line stands for the best approximation of all data, while the dashed and dotted lines represent relations (11) and (12), respectively, for the above zenith angle.

where $F_{\rm obs}$ is the flux measured under conditions of the real experiment and

$$\Delta\varepsilon = 12400(1/\lambda_1 - 1/\lambda_2) \approx 2.58 \text{ [eV]}. \qquad (17)$$

In the case being considered, we have $\lambda_1 = 3000$ Å and $\lambda_2 = 8000$ Å. The energy $E_{\rm el}$ is carried by the electron–photon component beyond the array plane. It was calculated by integrating the differential energy loss along the cascade curve $N_e(x)$ down to the

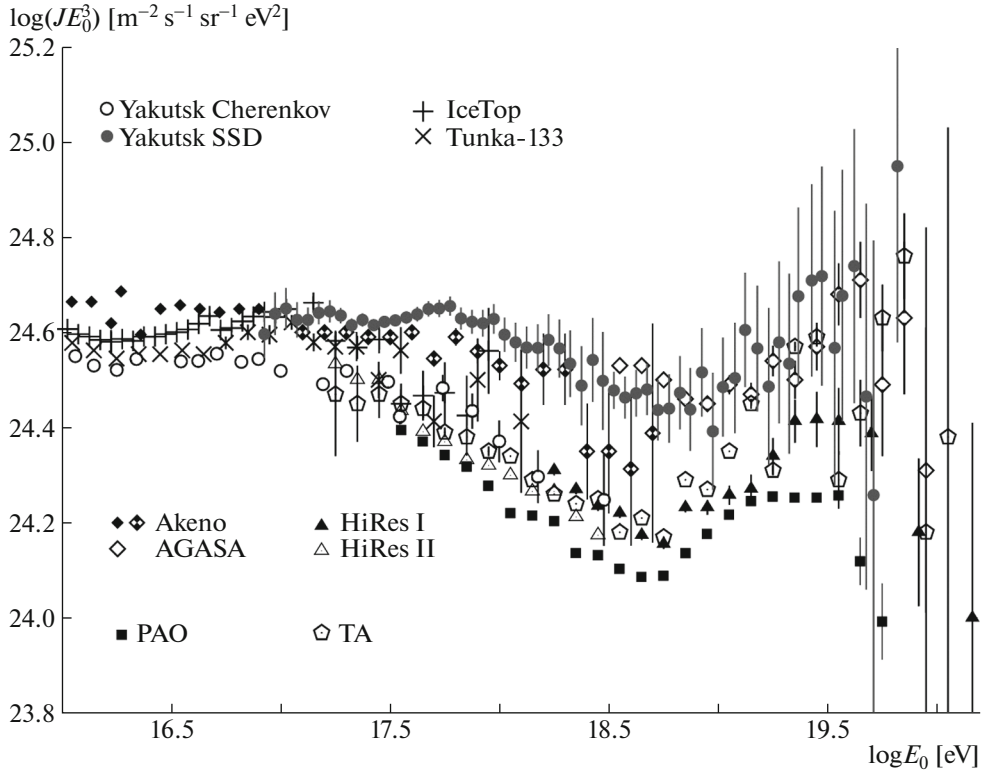

Fig. 6. Differential energy spectrum of cosmic rays according to data from various arrays: (closed and open circles) results obtained at the Yakutsk EAS array in the present study and in [26] from EAS Cherenkov radiation and (closed and half-closed diamonds) Akeno (1984, 1992) [27, 28], (open diamonds) AGASA [29], (inclined and right crosses) Tunka-133 [30] and IceTop [31], (closed and open triangles) HiRes I [32] and HiRes II [33], (closed boxes) PAO [7], and (pentagons) Telescope Array data.

observation level $X_{\rm obs}$; that is,

$$E_{\rm el} = \int\limits_{X_{\rm obs}}^{\infty} (dE/dx)_i N_e(x) dx \qquad (18)$$

$$\approx 2.2 \times 10^6 N_e(X_{\rm obs}) \int\limits_{X_{\rm obs}}^{\infty} \exp(X_{\rm obs} - x)/\lambda_a dx,$$

where $N_e(X_{\rm obs})$ is the number of electrons at the observation level. It was found from the relation

$$N_e(X_{\rm obs}) \approx \langle N_s(X_{\rm obs})\rangle - 1.8\langle N_\mu(X_{\rm obs})\rangle, \qquad (19)$$

where $\langle N_s(X_{\rm obs})\rangle$ and $\langle N_\mu(X_{\rm obs})\rangle$ are the average values of the total numbers of responses to, respectively, all particles and muons at a threshold above 1 GeV.

The muon energy E_μ was measured experimentally as

$$E_\mu \approx \langle E_{1\mu}\rangle\langle N_\mu(X_{\rm obs})\rangle, \qquad (20)$$

where $\langle E_{1\mu}\rangle = 10.6$ GeV is the average energy of one muon.

From the calculated values in Table 2 that were averaged over all models, it follows that the total value $E_i + E_{\rm el} + E_\mu$ is about 93% of the primary energy. Its remaining part, ΔE, is not controlled at the Yakutsk EAS array. It includes the neutrino energy transferred to nuclei in various reactions and the muon and hadron energy losses by atmosphere ionization. In [9, 10], its value was taken from earlier calculations. Roughly, it is compatible with the estimates obtained with the aid of the CORSIKA code [16].

The rightmost column of Table 2 contains the total values of all preceding components. The energy of $E_0 = 1.173 \times 10^{18}$ eV in the "Experiment" line exceeds its averaged model estimate $\langle E_0\rangle = 0.997 \times 10^{18}$ eV by a factor of about 1.177. This difference arose because of the use in [9, 10] of the coefficient $k = 3.7 \times 10^4$ eV/photon eV^{-1} overestimated in relation to its calculated value of $\langle k\rangle = 3.158 \times 10^4$ eV/photon eV^{-1}. The new estimate $E_0 = 1.019 \times 10^{18}$ eV obtained by means of the above calorimetric method with the refined values of $E_i = \langle k\rangle F$, $\langle E_{1\mu}\rangle = 10.3$ GeV, and ΔE in the lowermost line of Table 2. It is shown, along with other data from [9], in Fig. 5 (closed circles). The open circles in this figure represent data from [10] for which the values of F and $E_{\rm ion}$ were modified via refining the

transparency of the atmosphere and via employing the the new coefficient k (see Fig. 4). The solid line corresponds to the dependence

$$E_0 = (3.76 \pm 0.3) \times 10^{17} (S_{600}(0^\circ))^{1.02\pm0.02}\ [\text{eV}], \quad (21)$$

which complies with all experimental points upon rescaling $S_{600}(18.2^\circ)$ to a vertical direction according to Eq. (2) by employing the absorption length λ represented by the dashed curve in Fig. 3 (for a mixed composition of primary particles). The dashed and dotted lines in Fig. 5 correspond to relations (11) and (12), which characterize the applicability limits for the models of EAS development that were considered above. The QGSJET-01-d and SIBYLL-2.1 models provide the best agreement with experimental data.

3. PRIMARY ENERGY SPECTRUM

We have considered more than 10^6 showers detected over the period of continuous operation of the Yakutsk EAS array from 1974 to 2017. The spectrum was constructed on the basis of the procedure proposed in [25]. The energy of individual events was found according to the refined calorimetric formula (21), which depends only slightly on models of EAS development and which relies on results close to one another (see Table 2). The absorption ranges were taken from the calculations illustrated in Fig. 3 and performed for the real mixed composition of primary particles [23, 24]. In Fig. 6, the resulting spectrum is represented by closed circles. The open circles correspond to the spectrum obtained in [26] at the Yakutsk EAS array from EAS Cherenkov radiation. The closed, half-closed, and open diamonds stand for Akeno (1984, 1992) [27, 28] and AGASA [29] data. The inclined and right crosses represent the spectra obtained at, respectively, the Tunka-133 [30] and Ice Top [31] arrays. The closed and open triangles correspond to HiRes I [32] and HiRes II [33] data. The closed boxes stand for the PAO (Pierre Auger Observatory) spectrum [34].

Our spectrum agrees with the Akeno–AGASA spectra [27–29] within the experimental errors over the whole range of measured energies. Possibly, this is due to the use of similar scintillation detectors and similar data-analysis procedures in these two cases. Good agreement with Tunka-133 [30] and Ice Top [31] data is observed at $E_0 \approx 10^{17}$ eV. For $E_0 > 10^{18}$ eV, our results and the results obtained at HiRes [32, 33] and PAO [7] disagree substantially, possibly because of some special technical features of those arrays.

4. CONCLUSIONS

The application of the CORSIKA code to the Yakutsk EAS array made it possible to reanalyze critically its energy calibration, which has long been been the subject of lively discussions and disagreement with colleagues performing similar experiments at other arrays worldwide. This became possible owing to the availability of modern models of EAS development. Relying on these models, we were able to calculate responses of scintillation detectors and to obtain, on this basis, a set of possible estimates of the primary energy [see Eqs. (9)–(12)]. The calculations revealed that, in expressions (1) and (4), the energy scattered in the atmosphere in the form of an electromagnetic component is overestimated by 12% to 17%, depending on the shower-maximum depth $X_{\max}$ (Fig. 4); in Eq. (4), this difference is additionally aggravated by an overestimation of about 17% shifting the transparency of the atmosphere in the undesirable direction. The new calorimetric result for E_0 in (21) reduced its estimate in relation to that in (4) by a factor of about 1.28 and diminished substantially the intensity of the energy spectrum measured at the Yakutsk EAS array (Fig. 6).

ACKNOWLEDGMENTS

This work was supported by the Program of the Presidium of Russian Academy of Sciences High-Energy Physics and Neutrino Astrophysics and by the Russian Foundation for Basis Research (project no. 16-29-13019 ofi-m).

REFERENCES

1. D. M. Edge, A. C. Evans, H. J. Garmston, R. J. O. Reid, A. A. Watson, J. G. Wilson, and A. M. Wray, J. Phys. A **6**, 1612 (1973).
2. A. V. Glushkov, V. M. Grigoriev, M. N. Dyakonov, T. A. Egorov, V. P. Egorova, A. N. Efimov, N. N. Efimov, N. N. Efremov, A. A. Ivanov, S. P. Knurenko, V. A. Kolosov, A. D. Krasilnikov, I. T. Makarov, V. N. Pavlov, P. D. Petrov, M. I. Pravdin, et al., in *Proceedings of the 20th International Cosmic Ray Conference ICRC, Moscow, 1987,* Vol. 5, p. 494.
3. N. Sakaki (for the AGASA Collab.), in *Proceedings of the 27th International Cosmic Ray Conference ICRC, Hamburg, 2001,* Vol. 1, p. 333.
4. R. U. Abbasi (High Resolution Fly's Eye Collab.), astro-ph/0208301v3 (2002).
5. V. P. Egorova, A. V. Glushkov, A. A. Ivanov, S. P. Knurenko, V. A. Kolosov, A. D. Krasilnikov, I. T. Makarov, A. A. Mikhailov, V. V. Olzoev, M. I. Pravdin, A. V. Sabourov, I. Ye. Sleptsov, and G. G. Struchkov, Nucl. Phys. B Proc. Suppl. **136**, 3 (2004).
6. Y. Tsunesada (for the Telescope Array Collab.), arXiv: 1111.2507v1.

7. F. Salamido (for the Pierre Auger Collab.), arXiv: 1107.4809.
8. A. V. Glushkov and M. I. Pravdin, JETP Lett. **87**, 345 (2008). doi 10.1134/S0021364008070023
9. A. V. Glushkov, Cand. Sci. (Phys. Math.) Dissertation (Skobeltsyn Inst. Nucl. Phys. Moscow State Univ., Moscow, 1982).
10. A. V. Glushkov, M. N. D'yakonov, T. A. Egorov, and N. N. Efimov, Izv. Akad. Nauk SSSR, Ser. Fiz. **55**, 713 (1991).
11. T. A. Egorov (for the Yakutsk Collab.), in *Proceeding of the Tokyo Workshop on Techniques for the Study of Extremely High Energy Cosmic Rays, Tokyo, 1993*.
12. A. V. Glushkov, V. P. Egorova, A. A. Ivanov, S. P. Knurenko, V. A. Kolosov, A. D. Krasilnikov, I. T. Makarov, A. A. Mikhailov, V. V. Olzoyev, V. V. Pisarev, M. I. Pravdin, A. V. Sabourov, I. E. Sleptsov, and G. G. Struchkov, in *Proceedings of the 28th International Cosmic Ray Conference ICRC, Tsukuba, 2003,* Vol. 1, p. 389.
13. S. I. Nikolsky, in *Proceedings of the 5th International Seminar on Cosmic Rays, La Pas, 1962,* Vol. 2, p. 48.
14. A. V. Glushkov, M. I. Pravdin, and A. V. Saburov, JETP Lett. **99**, 431 (2014). doi 10.1134/S0021364014080086
15. A. V. Glushkov, M. I. Pravdin, and A. Sabourov, Phys. Rev. D **90**, 012005 (2014).
16. D. Heck, J. Knapp, J. N. Capdevielle, G. Schatz, and T. Thouw, *CORSIKA: A Monte Carlo Code to Simulate Extensive Air Showers,* FZKA 6019 (Forschungszentrum Karlsruhe, 1998).
17. A. V. Glushkov, O. S. Diminshtein, T. A. Egorov, N. N. Efimov, L. I. Kaganov, D. D. Krasil'nikov, S. V. Maksimov, V. A. Orlov, M. I. Pravdin, and I. E. Sleptsov, in *Proceedings of the Soviet Symposium on Experimental Methods of Very High Energy Cosmic Rays Research* (YaF SO AN SSSR, Yakutsk, 1974), p. 43.
18. N. N. Kalmykov, S. S. Ostapchenko, and A. I. Pavlov, Nucl. Phys. B Proc. Suppl. **52**, 17 (1997).
19. S. Ostapchenko, Phys. Rev. D **83**, 014018 (2011).
20. E.-J. Ahn, R. Engel, T. K. Gaisser, P. Lipari, and T. Stanev, Phys. Rev. D **80**, 094003 (2009).
21. T. Pierog, Iu. Karpenko, J. M. Katzy, E. Yatsenko, and K. Werner, arXiv: 1306.0121 [hep-ph].
22. G. Battistoni, F. Cerutti, A. Fassò, A. Ferrari, S. Muraro, J. Ranft, S. Roesler, and P. R. Sala, AIP Conf. Proc. **896**, 31 (2007).
23. A. V. Glushkov and A. V. Sabourov, JETP Lett. **100**, 695 (2015); doi 10.1134/S0021364014230052
24. A. Sabourov, A. Glushkov, M. Pravdin, Y. Egorov, A. Ivanov, S. Knurenko, V. Mokhnachevskaya, I. Petrov, and L. Timofeev, PoS(ICRC2017) 553 (2017).
25. A. V. Glushkov and M. I. Pravdin, JETP **101**, 88 (2005). doi 10.1134/1.2010665
26. S. Knurenko and A. Sabourov, EPJ Web **53**, 04004 (2013).
27. M. Nagano, T. Hara, Y. Hatano, N. Hayashida, S. Kawaguchi, K. Kamata, K. Kifune, and Y. Mizumoto, J. Phys. G **10**, 1295 (1984).
28. M. Nagano, M. Teshima, Y. Matsubara, H. Y. Dai, T. Hara, N. Hayashida, M. Honda, H. Ohoka, and S. Yoshida, J. Phys. G **18**, 423 (1992).
29. K. Shinozaki (AGASA Collab.), Nucl. Phys. B Proc. Suppl. **151**, 3 (2006).
30. S. F. Berezhnev, D. Besson, N. M. Budnev, A. Chiavassa, O. A. Chvalaev, O. A. Gress, A. N. Dyachok, S. N. Epimakhov, A. Haungs, N. I. Karpov, N. N. Kalmykov, E. N. Konstantinov, A. V. Korobchenko, E. E. Korosteleva, V. A. Kozhin, L. A. Kuzmichev, et al., arXiv: 1201.2122v1.
31. IceCube Collab. (M. G. Aartsen et al.), arXiv: 1307.3795v1.
32. Y. Tsunesada (on behalf of the Telescope Array Collab.), arXiv: 1111.2507v1.
33. Z. Zundel (for Telescope Array Collab.), PoS(ICRC2015)445 (2015).